JACS
JOURNAL OF THE AMERICAN CHEMICAL SOCIETY
Article
pubs.acs.org/JACS

Empirical and Theoretical Insights into the Structural Features and Host–Guest Chemistry of M_8L_4 Tube Architectures

Wenjing Meng,[†,§] Aaron B. League,[‡] Tanya K. Ronson,[†] Jack K. Clegg,[†,∥] William C. Isley, III,[‡] David Semrouni,[‡] Laura Gagliardi,*[,‡] Christopher J. Cramer,*[,‡] and Jonathan R. Nitschke*[,†]

[†]Department of Chemistry, University of Cambridge, Lensfield Road, Cambridge, CB2 1EW, U.K.

[‡]Department of Chemistry, Chemical Theory Center, and Supercomputer Institute, University of Minnesota, 207 Pleasant Street SE, Minneapolis, Minnesota 55455, United States

Supporting Information

ABSTRACT: We demonstrate a general method for the construction of M_8L_4 tubular complexes via subcomponent self-assembly, starting from Cu^I or Ag^I precursors together with suitable elongated tetraamine and 2-formylpyridine subcomponents. The tubular architectures were often observed as equilibrium mixtures of diastereomers having two different point symmetries (D_{2d} or $D_2 \rightleftarrows D_4$) in solution. The equilibria between diastereomers were influenced through variation in ligand length, substituents, metal ion identity, counteranion, and temperature. In the presence of dicyanoaurate(I) and Au^I, the D_4-symmetric hosts were able to bind linear $Au(Au(CN)_2)_2^-$ (with two different configurations) as the best-fitting guest. Substitution of dicyanoargentate(I) for dicyanoaurate(I) resulted in the formation of $Ag(Au(CN)_2)_2^-$ as the optimal guest through transmetalation. Density functional theory was employed to elucidate the host–guest chemistries of the tubes.

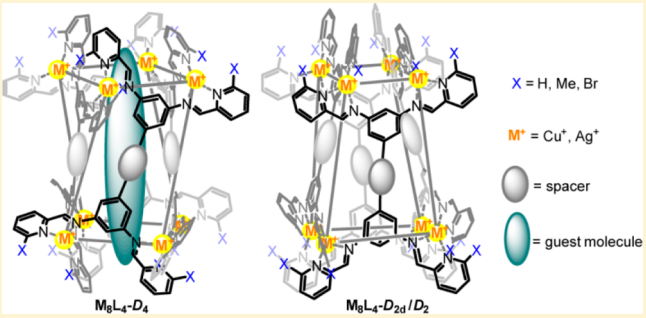

INTRODUCTION

Metal–organic container molecules[1−7] have attracted interest due to their ability to isolate guest molecules in the microenvironments provided by their internal cavities. Encapsulation may alter the chemical behavior of a guest,[8] leading to applications in catalysis,[9−14] sensing,[15−20] stabilization,[21−25] and transport.[26−29] Subcomponent self-assembly, wherein dynamic-covalent C═N[30,31] and coordinative M → L bonds are formed during the same overall process,[32−35] has proven particularly useful for the synthesis of metal–organic hosts.[36] The first such hosts had tetrahedral[37−41] or cubic[42−46] structures, with approximately spherical cavities suitable for binding compact anions and small molecules.

Newer subcomponent-self-assembled hosts have been prepared that have yet more complex structures, including pseudoicosahedra,[47] hexagonal[48,49] and pentagonal[50] prisms, twisted cubes,[51] asymmetric structures,[52] and tubular architectures.[53] Tubes represent interesting research targets due to their potential biomimetic function as molecular channels for selective transportation of ions and molecules, and as hosts for linear guests. Although many tubular organic systems have been reported,[54−59] the structural properties and host–guest chemistries of discrete metal–organic tubes have been less well-studied.[60,61]

Recently, we have reported the assembly of M_8L_4 tubular capsule **1a** from the reaction of tetraamine **A**, 6-methyl-2-formylpyridine **1** and $[Cu(MeCN)_4]BF_4$ (Scheme 1).[53] This tube is able to transform $Au(CN)_2^-$ into a linear complex anion

Scheme 1. General Synthesis of M_8L_4 Tubes

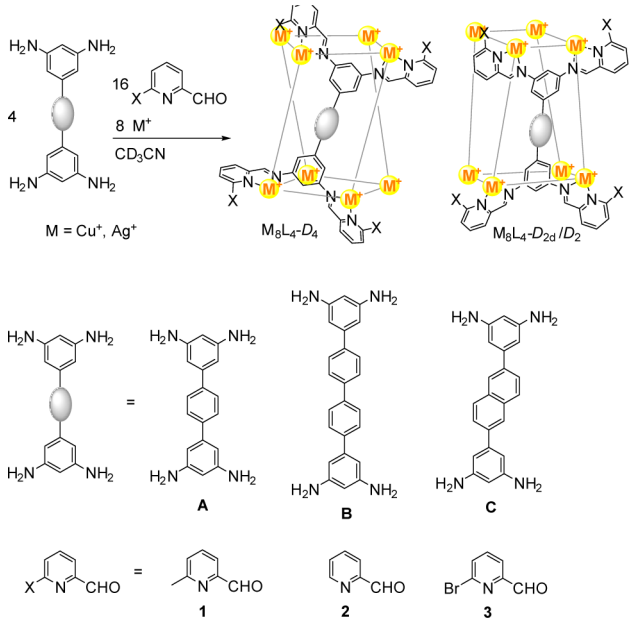

NC-Au-CN-Cu-NC-Au-CN^-, which was not independently observed, as the optimal guest for encapsulation. Building upon

Received: December 20, 2013
Published: January 21, 2014

   dx.doi.org/10.1021/ja412964r | J. Am. Chem. Soc. 2014, 136, 3972−3980

our previous work on tube **1a**, we demonstrate how the length, shape and substituents of the ligands, the counteranions and metals can influence the stereochemistry and host–guest chemistry of the tubular complexes. Insights into the nature and origin of some of these processes are provided by density functional theory (DFT) analysis.

RESULTS AND DISCUSSION

Synthesis and Stereochemistry. A M_8L_4 tubular complex can be constructed as the uniquely observed product using elongated tetraamine **A**, **B**, or **C** (4 equiv), 2-pyridinecarboxaldehyde derivatives (16 equiv), and a suitable salt of Cu^I or Ag^I (8 equiv) in acetonitrile, as depicted in Scheme 1. Depending on the orientation of the bidentate iminopyridine binding sites, the M_8L_4 tube can adopt approximate $D_{2d}(/D_2)$ or D_4 point symmetries where the metal ions define the vertices of a cuboid. As we observed earlier,[53] in the crystal structures of tube **1a**·BF_4, the D_{2d} isomer has isosceles trapezoids as the long faces of the cuboid, with the shorter faces forming rectangles, whereas in the D_4 isomer the cuboid approximates a right square prism in which one of the square faces is twisted with respect to the other. The D_4 isomer possesses a narrow linear channel that is capable of trapping two acetonitrile molecules inside. The difference in the symmetry of the two diastereomers led to characteristic NMR peak multiplicities, allowing them to be distinguished by ^{1}H NMR. The population of the two isomers in solution reflects their relative thermodynamic stability, which can be tuned in several ways, as summarized in Table 1.

Table 1. Summary of Isomers Formed in Acetonitrile upon the Variation of Tetraamine, Aldehyde, and Counter Ion for Cu_8L_4 Tubes

			counter ion	
complex	tetraamine	aldehyde	BF_4^-	PF_6^-
1a	**A**	**1**	D_4:D_{2d} 90:10%	D_4 only
2a		**2**	D_{2d} only	D_4:D_{2d} 52:48%
3a		**3**	D_{2d} only	unstable
1b	**B**	**1**	D_4:D_{2d} 1:99%	D_4:D_{2d} 24:76%
1c	**C**	**1**	D_2 only	D_4:D_2 6:94%

The substituent on the aldehyde subcomponent was observed to influence the stability of the tube isomers. Replacing a methyl group with a proton (aldehyde **2**) or a bromine (aldehyde **3**) at the 6 position of pyridine-2-carboxaldehyde resulted in the relative destabilization of the D_4-symmetric isomer, so that in the cases of **2a**·BF_4, **3a**, and **1c**·BF_4, the D_4 isomer did not form in solution.

In most cases, both BF_4^- and PF_6^- counterions allow the formation of M_8L_4 tubes, and the formation of the D_4 isomer is preferred when PF_6^- is present. The crystal structure of **2a**-D_4·PF_6 (Figure 1) reveals that one PF_6^- anion is located at each end of the tube with one fluorine atom pointing directly into the channel, and four such anions associate at the junctions between two neighboring terphenyl ligands, which are also sandwiched between two pyridine residues. For all these anions, short contacts (2.3–2.8 Å) are observed between fluorine atoms and protons of the complex, which may account for the extra stabilization effect brought by the PF_6^- anion.[62,63]

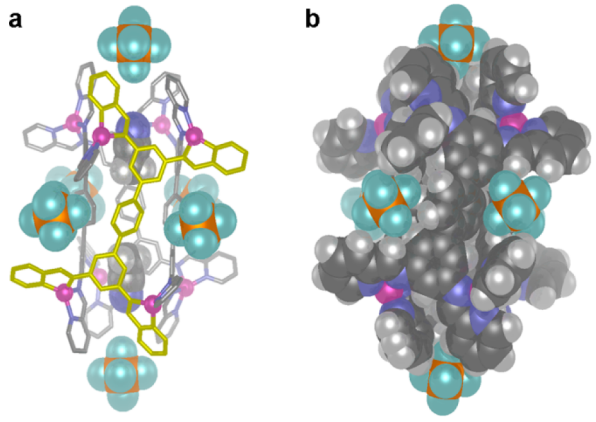

Figure 1. Crystal structure of **2a**-D_4·PF_6. (a) Representation of the complex with one ligand highlighted in yellow (hydrogen atoms not shown). (b) CPK representation showing the proximity between PF_6^- anions and ligand hydrogens.

Host **2a**·PF_6 has an approximately equal distribution of both isomers in solution. The interconversion between **2a**-D_4·PF_6 and **2a**-D_{2d}·PF_6 could be followed by ^{1}H NMR spectroscopy as the temperature was varied. Kinetic studies (described in the Supporting Information) revealed $\Delta H^{\ddagger} = 108 \pm 7$ kJ mol^{-1} and $\Delta S^{\ddagger} = 71 \pm 24$ J K^{-1} mol^{-1} for the isomerization from **2a**-D_4·PF_6 to **2a**-D_{2d}·PF_6, and $\Delta H^{\ddagger} = 58 \pm 8$ kJ mol^{-1}, and $\Delta S^{\ddagger} = -104 \pm 24$ J K^{-1} mol^{-1} for the reverse transformation (from **2a**-D_{2d}·PF_6 to **2a**-D_4·PF_6), which appears more entropically disfavored compared to the same process for the terphenyl congener **1a**·BF_4 ($\Delta S = -62 \pm 21$ J K^{-1} mol^{-1}).[53] The rate constants for both transformations were identical at 283 K, marking **2a**-D_4 as the dominant species in solution below this temperature, and **2a**-D_{2d} above.

Since the choice of counterions has been shown to have a measurable but small impact on the stereochemistry of almost all of the complexes listed in Table 1, a computational study was undertaken to determine the differential effect of including two PF_6^- counterions at the ends of the empty D_4 versus the D_{2d} isomers of **1a**. A relative stabilization of the D_{2d} isomer by only 4.1 kJ mol^{-1} was computed (see Computational Methods section for theory details), a value commensurate with the small energy changes associated with the variations in isomeric ratios discussed above.

Longer ligands also disfavored the D_4 isomer: the reaction between tetraamine **B** or **C**, 6-methyl-2-pyridine-carboxaldehyde **1** and $[Cu(MeCN)_4]BF_4$ in acetonitrile produced **1b**-D_{2d} and **1c**-D_2 as the predominant isomers, respectively (Figures S27 and S33, Supporting Information). The hexafluorophosphate anion was again found to slightly stabilize the D_4 isomer; when copper(I) hexafluorophosphate was used in place of the tetrafluoroborate, the equilibrium ratios were found to be 24:76% and 6:94% for complexes **1b**-D_4:**1b**-D_{2d} and **1c**-D_4:**1c**-D_2, respectively, as revealed by their ^{1}H NMR spectra (Figures S21 and S30, Supporting Information). Models suggested that the D_4-symmetric tubes constructed from tetraamine **B** or **C** are not long enough to accommodate a third acetonitrile molecule inside the channel, leaving instead additional empty space, and incurring an energetic penalty for doing so. Single crystals of **1b**·BF_4 and **1c**·PF_6 were isolated by vapor diffusion of diethyl ether (or diisopropyl ether) into an acetonitrile solution of the

dx.doi.org/10.1021/ja412964r | J. Am. Chem. Soc. 2014, 136, 3972–3980

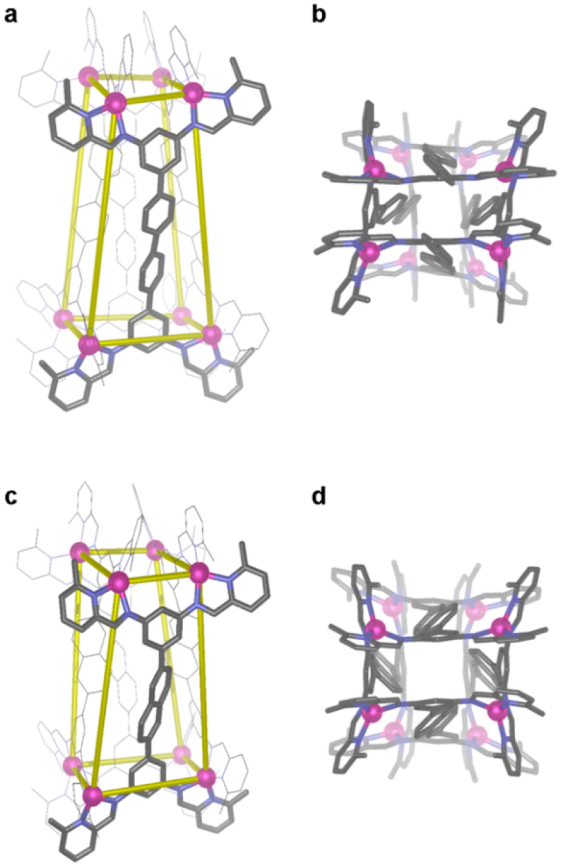

Figure 2. Crystal structures of **1b**-D_{2d}·BF_4 (a,b) and **1c**-D_2·PF_6 (c,d).[64] (a,c) Side view; (b,d) top view. Hydrogen atoms, solvent molecules, and counterions are omitted for clarity.

respective complexes. X-ray analyses revealed the presence of **1b**-D_{2d} (Figure 2a,b) and **1c**-D_2 (Figure 2c,d), whose structures resemble that of **1a**-D_{2d}. For **1b**-D_{2d} the elongation of the ligand backbone from terphenylene to quaterphenylene did not result in an increase of the width of the tube channel, but rather narrows it. The shorter faces (Figure 2b) are slightly distorted from a rectangular geometry. The average Cu−Cu distance of the shorter edge of the top and bottom faces was 5.3 Å, 0.1 Å shorter than in **1a**-D_{2d}. For **1c**-D_2 the presence of a naphthalene spacer reduces the symmetry of the complex by removing the mirror plane that bisects the ligand. The naphthalene spacer also introduces an offset between the two terminal phenyl rings, which slightly widens the tube channel. The shorter edge of the rectangular face in **1c**-D_2 (5.6 Å) is 0.2 Å longer than that in **1a**-D_{2d}.

Ag^I can also be used in place of Cu^I to form an M_8L_4 tube. The reaction between tetraamine **A**, 6-methyl-2-pyridinecarboxaldehyde **1** and $AgBF_4$ in acetonitrile produced **4**-D_{2d} as the only observed product in solution, as verified by ^1H NMR and MALDI-MS. Doublets were observed for the two symmetry-independent imine protons, with J = 5.9 and 7.8 Hz due to the coupling between $^{107/109}Ag$ and the imine protons. Vapor diffusion of diethyl ether into an acetonitrile solution of **4**-D_{2d}·BF_4 allowed the isolation of single crystals suitable for X-ray analysis. The solid state structure reveals an approximate D_{2d}-symmetric M_8L_4 topology, consistent with solution observations (Figure 3). Compared to analogous Cu^I tubes (**1a**-D_{2d}, **1b**-D_{2d} and **1c**-D_2) **4**-D_{2d}·BF_4 is more distorted: the top view of **4**-D_{2d}·BF_4 shows that the shorter faces of the complex form a

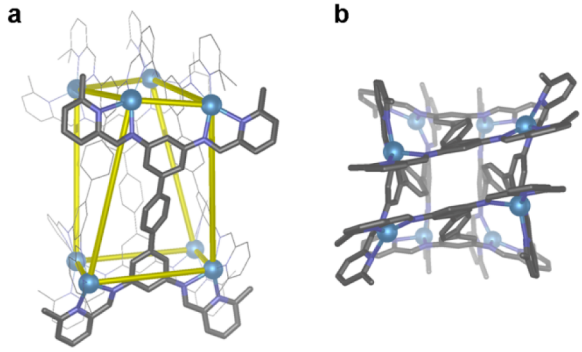

Figure 3. Crystal structure of Ag^I complex **4**-D_{2d}·BF_4. (a) Side view highlighting one ligand in thicker stick presentation. (b) Top view showing the distortion at the Ag^I centers.

parallelogram (Figure 3b), whereas those in the Cu^I tubes approximate a rectangle. Furthermore the Ag^I centers in **4**-D_{2d}·BF_4 show a greater degree of distortion from idealized tetrahedral geometry compared to the Cu^I centers in **1a**-D_{2d}·BF_4 with N−Ag−N angles in the range 72−154° compared N−Cu−N angles of 79−138° in its Cu^I analogue.

Host−Guest Chemistry. In previous work, we demonstrated that tube **1a**-D_4·BF_4 is capable of binding the complex anion $Cu(Au(CN)_2)_2^-$. The Cu^I ion bridges the two NC-Au-CN^-, and it could be substituted by Ag^I to give the $Ag(Au(CN)_2)_2^-$ adduct of **1a**-D_4·BF_4.

We have since determined DFT binding energies for these guests, and for every analogous guest with a different combination of central group-11 metal and dicyano group-11-metalate, inside of **1a** in acetonitrile continuum solvent. The results are shown in Table 2. Counterions were not included. Because of

Table 2. Computed Energies of Incorporation of Group-11 Metal Centers (Rows) And Dicyano Ends (Columns) In kJ mol^{-1}

central cation	peripheral anions in N≡C−M′−C≡N−M−N≡C−M′−C≡N		
	$Cu(CN)_2^-$	$Ag(CN)_2^-$	$Au(CN)_2^-$
D_4-host			
Cu^I	−36.8	−52.7	−69.0
Ag^I	−41.8	−53.1	−72.4
Au^I	−116.3	−129.3	−143.9
D_{2d}-host			
Cu^I	[a]	[a]	2.9
Ag^I	[a]	[a]	−15.1
Au^I	[a]	[a]	−97.9

[a]These values were not determined; no such binding is observed experimentally.

the high computational cost of optimizing the geometry of the large host−guest complexes, energies were not computed for the experimentally unobserved binding of the dicyanoargentate and dicyanocuprate guests in the D_{2d} host isomer.

Binding energies were calculated by determining the difference in energy between each host−guest complex and its corresponding separated starting compounds and acetonitrile-filled D_4 host isomer at 5 μM concentrations of the host−guest complexes. For consistency with the experimental conditions employed (vide infra), free Au^I was modeled as the cationic moiety of the salt $Au(tmbn)_2SbF_6$ (tmbn = 2,4,6-trimethoxybenzonitrile), whereas

dx.doi.org/10.1021/ja412964r | J. Am. Chem. Soc. 2014, 136, 3972−3980

free Cu^I and Ag^I were modeled as the tetrakis(acetonitrile) complexes.

The computed energies of binding matched the experimentally observed trend, where guests bound more strongly in the D_4 isomer and larger group-11 metals bound more strongly than smaller ones. This trend is consistent, allowing for reasonable extrapolation to the binding of the $Ag(CN)_2^-$ and $Cu(CN)_2^-$ guests in the D_{2d} host isomer. It is important to note that these energies of the host–guest complexes are relative to those of the solvent-filled cage and guest precursors, not the polymeric precipitate actually observed when no host is present. This distinction is likely to explain why we still obtain negative binding energies for the $Cu(Ag(CN)_2)_2^-$ and $Ag(Ag(CN)_2)_2^-$ guests, which are not observed to bind in situ, as these energies were not calculated relative to the global energy minimum.

Contrary to our previous inference,[53] it seems that the trend of favoring heavier group-11 metals at the center of the complex anion is predicated not upon increased cation-π interaction with the organic linkers of the host cage, but upon stronger intraguest binding. Figure 4 shows the DFT energetics

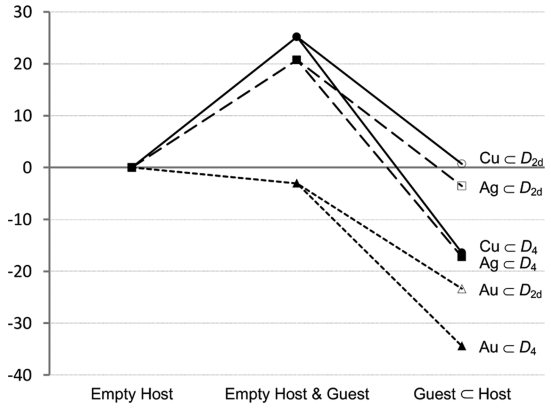

Figure 4. Calculated energetics for stepwise formation and incorporation of group-11 metal-centered bis-dicyanoaurates into **1a**-D_4 ("Guest ⊂ Host" data from last column of Table 2, "Empty Host" for guests as their dissociated precursors).

of the stepwise formation and insertion of the bis-dicyanoaurate guests into both **1a**-D_4 and **1a**-D_{2d}. For this hypothetical pathway, the global minimum energy of complex **1a** was assumed to be the D_4 isomer with two incorporated acetonitrile guests, and consequently this structure was chosen as the starting material for the host cage in the second step of the pathway. By comparing the energies of guest formation to those of host–guest complexation, the role of the comparatively strong gold–nitrogen bonds in stabilizing the $[Au(Au(CN)_2)_2 \subset$ **1a**-$D_4]$ complex becomes apparent.

In keeping with our theoretical predictions, the addition of $Au(tmbn)_2SbF_6$ (1.2 equiv) to $[Cu(Au(CN)_2)_2 \subset$ **1a**-$D_4{\cdot}BF_4]$ (1 equiv) led to the formation of a new host–guest complex $[Au(Au(CN)_2)_2 \subset$ **1a**-$D_4{\cdot}BF_4]$ (Scheme 2), as verified by ESI-MS. A low resolution crystal structure was obtained for the product, showing that Au^I replaced Cu^I as the bridging cation within the guest.

NMR spectra of $[Au(Au(CN)_2)_2 \subset$ **1a**-$D_4{\cdot}BF_4]$ revealed additional splitting: many ^1H signals appeared as a set of three closely spaced peaks of roughly equal intensity. Using isotopically labeled $KAu(^{13}CN)_2$, in the ^{13}C NMR spectrum (Figure S37, Supporting Information) the ^{13}C-labeled guest

Scheme 2. Formation of Trigold Host–Guest Complex $[Au(Au(CN)_2)_2 \subset$ 1a-$D_4]{\cdot}BF_4$ via Transmetalation[a]

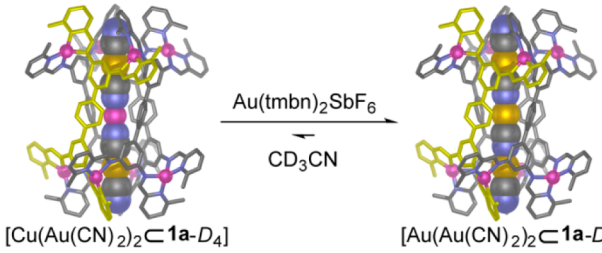

[a]The two representations shown are X-ray crystal structures. One configuration of the trigold guest is shown.

gave rise to three doublets and four singlets with different intensity, indicating the presence of multiple carbon environments.

The ^{13}C NMR spectra of the labeled host–guest complexes $[Cu(Au(^{13}CN)_2)_2 \subset$ **1a**-$D_4]$ and $[Ag(Au(^{13}CN)_2)_2 \subset$ **1a**-$D_4]$ exhibited a pair of characteristic doublets with J_{C-C} = 47 Hz for the guest signals, consistent with conservation of the NC-Au-CN aurocyanide configurations within the complex anion guests. Similar signals were not observed in the ^{13}C NMR spectrum for $[Au(Au(^{13}CN)_2)_2 \subset$ **1a**-$D_4]$. This observation indicates that in $[Au(Au(CN)_2)_2 \subset$ **1a**-$D_4]$, the guest configuration is different from that in $[Cu(Au(^{13}CN)_2)_2 \subset$ **1a**-$D_4]$ and $[Ag(Au(^{13}CN)_2)_2 \subset$ **1a**-$D_4]$. We thus infer that the conformation NC-Au-CN-Au-NC-Au-CN^- is not adopted by the guest in $[Au(Au(CN)_2)_2 \subset$ **1a**-$D_4]$. Our data were consistent with the guest adopting the conformations NC-Au-CN-Au-CN-Au-CN^- and NC-Au-NC-Au-CN-Au-CN^-, in which each gold(I) center is bonded to at least one carbon atom.

DFT calculations of the relative energies of the free complex anions in continuum acetonitrile solvent predict NC-Au-CN-Au-CN-Au-CN^- and NC-Au-NC-Au-CN-Au-CN^- to be more stable than NC-Au-CN-Au-NC-Au-CN^- by 15.5 and 14.6 kJ mol^{-1}, respectively. Thus, to have one gold atom *not* coordinated by at least one cyanide carbon atom is disfavored energetically. In so far as only two complex anion isomers are predicted to dominate in the absence of encapsulation, and assuming that binding energies are similar for the different complex anion isomers, upon guest binding we expect to observe close to a 2:1 statistical distribution of NC-Au-CN-Au-CN-Au-CN^-, and NC-Au-NC-Au-CN-Au-CN^-. We thus infer the tripling of host signals in the NMR to result from *one* set of signals associated with binding of NC-Au-NC-Au-CN-Au-CN^- and *two* sets of signals associated with binding of the asymmetric complex anion NC-Au-CN-Au-CN-Au-CN^-, which results in desymmetrization of the two ends of the tube. The presence of multiple conformations is mirrored in the solid-state behavior of group-11 cyanides.[65]

The titration of $Au(tmbn)_2SbF_6$ into an acetonitrile solution of $[Cu(Au(CN)_2)_2 \subset$ **1a**-$D_4{\cdot}BF_4]$ allowed the stability constant of 1.6×10^{11} M^{-3} for $[Au(Au(CN)_2)_2 \subset$ **1a**-$D_4{\cdot}BF_4]$ to be determined, 129 times greater than that of $[Cu(Au(CN)_2)_2 \subset$ **1a**-$D_4{\cdot}BF_4]$ and 3.7-fold higher than $[Ag(Au(CN)_2)_2 \subset$ **1a**-$D_4{\cdot}BF_4]$.

Tetraphenyl tube **1b**·PF_6 did not form any host–guest complex in the presence of $KAu(CN)_2$, which suggests the energy gained by trapping the guest $Cu(Au(CN)_2)_2^-$ is not enough to compensate energy lost during isomerization from **1b**-D_{2d} to **1b**-D_4. In contrast, for naphthalene-based tube **1c**·PF_6 the addition of $KAu(CN)_2$ resulted in a rapid and clean

dx.doi.org/10.1021/ja412964r | J. Am. Chem. Soc. 2014, 136, 3972–3980

Scheme 3. Formation of Host–Guest Complexes from 1c·PF_6.[a]

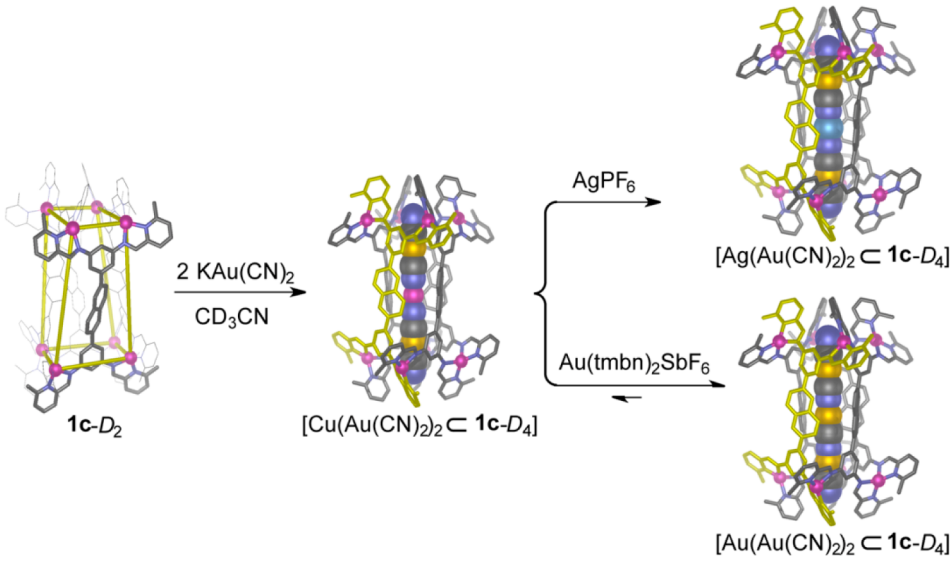

[a] $[Cu(Au(CN)_2)_2 \subset$ **1c**-$D_4]$ Is Shown as the X-ray Crystal Structure.

transformation to $[Cu(Au(CN)_2)_2 \subset$ **1c**-$D_4]$ (Scheme 3), despite the low abundance of **1c**-D_4 in solution. The crystal structure of the product confirmed the encapsulation of $Cu(Au(CN)_2)_2^-$ within **1c**-D_4, consistent with NMR and ESI-MS observations. The central Cu^I within the guest could be replaced by Ag^I or Au^I in a similar way to the analogous terphenyl tube $[Cu(Au(CN)_2)_2 \subset$ **1a**-$D_4]$ (Scheme 3).

Linear dicyanoargentate, $Ag(CN)_2^-$, has very similar dimensions to $Au(CN)_2^-$, yet no host–guest complex formation was observed when **1a**·PF_6 was treated with $Ag(CN)_2^-$ in the presence of either Cu^I or Ag^I. In contrast, when Au^I was added, a new D_4-symmetric complex was rapidly generated. This new product was not the expected $[Au(Ag(CN)_2)_2 \subset$ **1a**-$D_4]\cdot PF_6$, but a transmetalated product $[Ag(Au(CN)_2)_2 \subset$ **1a**-$D_4]\cdot PF_6$, as verified by NMR and ESI-MS (Scheme 4). In the absence

Scheme 4. Formation of $[Ag(Au(CN)_2)_2 \subset$ 1a-$D_4]\cdot PF_6$ via Transmetalation between $Ag(CN)_2^-$ and Au^I

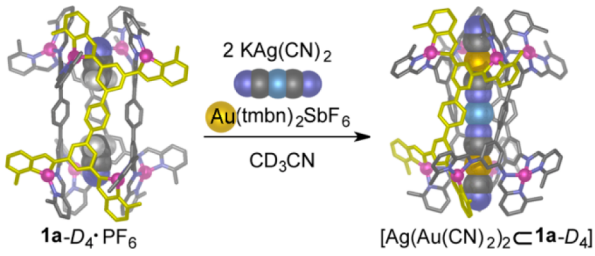

of the host **1a**·PF_6, mixing $Ag(CN)_2^-$ with Au^I resulted in the formation of white precipitate, which we infer to be the polymeric mixed-metal cyanide.[66,67] Host **1a**·PF_6 therefore acts as a solubilizing carrier, allowing the encapsulated guest to be studied using routine spectroscopic methods.

The lack of observed binding of $[Au(Ag(CN)_2)_2]^-$ in **1a** can be explained computationally. DFT calculations show that while the fully formed guest $Au(Ag(CN)_2)_2^-$ is predicted to bind to **1a**-D_4 *more* strongly than $Ag(Au(CN)_2)_2^-$ (by 56.9 kJ mol^{-1}, see Table 2), the transmetalation of dicyanoargentate to dicyanoaurate by the pathway

$$Ag(CN)_2^- + Au(tmbn)_2^+ + 4CH_3CN \rightarrow Au(CN)_2^- + Ag(CH_3CN)_4^+ + 2tmbn$$

is predicted to be exoergic by 146.4 kJ mol^{-1}, making the $[Ag(Au(CN)_2)_2 \subset$ **1a**-$D_4]$ complex more enthalpically favorable than its gold bis-dicyanoargentate counterpart by 235.6 kJ mol^{-1}.

CONCLUSION

In this study we have developed a general synthetic procedure for M_8L_4 tubular complexes using tetraamines with two 3,5-diaminophenylene moieties connected by a suitable spacer. This technique allows facile investigations into the influences of subtle changes in any of the subcomponents on the complex structure. The M_8L_4 tubes are present in solution as either D_4-symmetric or D_{2d}/D_2-symmetric isomers, which are in dynamic equilibrium. The D_4 isomer, which is the only one observed to bind guests, is more stabilized when PF_6^- is present as the counteranion, whereas the D_{2d}/D_2 isomer is stabilized by the elongation of the ligand or the introduction of an offset between tube termini. Further systemic adaptation is revealed in the host–guest chemistry of the tubes. Dicyanoaurate is a necessary subcomponent of all guests that we observe to be bound by any tube, and the system will undertake to transform guests in order to achieve an optimal host–guest complex through guest recombination or transmetalation. This work therefore builds upon and contributes to fundamental studies of systems chemistry,[68] specifically the dynamic response of a system to external stimuli, as is required in the design and creation of increasingly complex molecular machines.[69−73] The design of a system that is specifically adapted to bind gold cyanides may also be of relevance to the mining industry,[74] and the ability to specifically bind linear guests may allow for their catalytic transformation, as has been observed in other systems.[9−14]

EXPERIMENTAL SECTION

Computational Methods. All calculations employed the PBE-D3[75,76] functional as implemented in the ADF 2013 software package.[77−79] TZP basis sets with large frozen cores were employed for metal atoms, and DZP basis sets for the organic linkers.[80]

dx.doi.org/10.1021/ja412964r | J. Am. Chem. Soc. 2014, 136, 3972−3980

The zero-order regular approximation (ZORA) was employed to account for scalar relativistic effects.[81−83]

Empty cages and host−guest complexes were first optimized in the gas phase, and final energies were computed from single-point calculations on these minima including acetonitrile solvation effects computed from the COSMO continuum solvent model.[84] When representative host−guest complexes were subjected to reoptimization including solvation effects, their energies were observed to fluctuate but not to decrease (or converge, because of apparent numerical noise), on which basis we concluded that for the large cage structures, solvated single-point calculations on gas-phase geometries were sufficiently accurate for our purposes. The geometries of small molecule guests and guest precursors, however, were optimized including acetonitrile solvation effects. Because of the size of the host structures, no frequency calculations were performed, and consequently the theoretical energies reported in this paper include no thermal corrections.

General Methods. Unless otherwise specified, all starting materials were purchased from commercial sources and used as supplied. Chromatographic separations were performed on silica gel 60 (particle size: 0.040−0.063 mm) purchased from Aldrich. TLC was performed on silica gel 60 F254 plates purchased from Merck and visualized under ultraviolet light (254 nm). NMR spectra were recorded on a Bruker DRX-400 and Bruker Avance 500 Cryo. Chemical shifts (δ) are reported in parts per million (ppm) and are reported relative to acetonitrile-d_3 at 1.94 ppm at 298 K unless otherwise noted. Low resolution electrospray ionization mass spectra (ESI-MS) were obtained on a Micromass Quattro LC, infused from a Harvard Syringe Pump at a rate of 10 μL per minute. MALDI was carried out by the EPSRC National MS Service Centre at Swansea. Building blocks [1,1′:4′,1″-terphenyl]-3,3″,5,5″-tetraamine **A** and $Au(tmbn)_2SbF_6$ were synthesized following literature procedures.[53,85]

Synthesis and Characterization of Metal Complexes. 1a·PF_6. To a Schlenk tube was added **A** (80 mg, 27.5 mmol, 4 equiv), 6-methyl-2-pyridinecarboxaldehyde (133.5 mg, 110.2 mmol, 16 equiv), $Cu(CH_3CN)_4PF_6$ (205 mg, 55.1 mmol, 8 equiv) and acetonitrile (15 mL). The solution was degassed by three evacuation/nitrogen fill cycles and stirred at room temperature for 12 h. A dark pink solution resulted. The desired product **1a**·PF_6 was precipitated by adding diethyl ether into the reaction mixture, and was isolated by filtration as a black solid (200 mg, 65%): ^{1}H NMR (CD_3CN, 500 MHz) 9.31 (8H, s, imine *H*), 8.59 (8H, t, *J* 8.00, py-*H*), 8.07−8.05 (16H, d, py-*H*), 7.91 (8H, d, *J* 8.00, py-*H*), 7.77 (8H, d, *J* 7.50, py-*H*), 7.67 (8H, m, py-*H*), 7.65 (8H, s, Ph-*H*), 7.63 (8H, s, imine *H*), 6.89 (16H, s, Ph-*H*), 6.82 (16H, s, Ph-*H*), 2.52 (24H, s, CH_3), 2.44 (24H, s, CH_3); ^{13}C {^{1}H} NMR (CD_3CN, 125 MHz) 162.50, 161.38, 161.02, 159.35, 150.87, 150.31, 150.20, 149.99, 143.82, 140.44, 139.67, 139.64, 131.57, 130.23, 128.55, 127.80, 126.99, 123.55, 115.42, 26.42, 25.88; ESI-MS $[\mathbf{1a}(PF_6)_2]^{6+}$ 601.76, $[\mathbf{1a}(PF_6)_3]^{5+}$ 751.08, $[\mathbf{1a}(PF_6)_4]^{4+}$ 975.15, $[\mathbf{1a}(PF_6)_5]^{3+}$ 1348.58. Found: C, 48.60; H, 3.48; N, 9.80%. Calc. for $C_{184}H_{152}Cu_8F_{48}N_{32}P_8{\cdot}3H_2O$: C, 48.75; H, 3.51; N, 9.89%.

2a·PF_6. To a Schlenk tube was added **A** (10 mg, 34.4 μmol, 4 equiv), 2-pyridinecarboxaldehyde (13.1 μL, 0.13 mmol, 16 equiv), $Cu(CH_3CN)_4PF_6$ (25.6 mg, 68.8 mmol, 8 equiv) and acetonitrile (5 mL). The solution was stirred at room temperature for 12 h to give a dark pink solution. Diethyl ether was added into the reaction mixture; the resulting mixture was centrifuged, and the solvent was decanted. The solid was dried under a vacuum to give the desired product **2a**·PF_6 as dark pink solid (16.6 mg, 45%): ^{1}H NMR (CD_3CN, 500 MHz) 9.67 (8H, br, imine *H*), 9.33 (8H, s, imine *H*), 9.29 (8H, s, imine *H*), 8.87 (8H, d, *J* 4.70, Ar-*H*), 8.65 (8H, dt, *J* 7.90, 1.25, py-*H*), 8.62 (8H, d, *J* 4.85, Ar-*H*), 8.30−7.89 (24H, Ar-*H*), 7.80 (8H, s, Ph-*H*), 7.75 (8H, t, *J* 6.43, py-*H*), 7.65 (8H, s, Ph-*H*), 7.60 (8H, t, *J* 5.78, py-*H*), 7.56 (8H, br, py-*H*), 7.65 (8H, s, Ph-*H*), 7.19 (8H, d, *J* 1.25, Ph-*H*), 7.00 (8H, d, *J* 7.85, Ph-*H*), 6.97 (8H, s, Ph-*H*), 6.94 (8H, s, Ph-*H*), 6.84 (8H, s, Ph-*H*), 6.71 (8H, d, *J* 7.80, Ph-*H*); ^{13}C {^{1}H} NMR (CD_3CN, 125 MHz) 162.57, 162.20, 160.82, 159.05, 151.94, 151.64, 151.52, 151.41, 151.21, 150.76, 150.32, 150.19, 149.95, 149.75,147.81,144.97, 144.08, 143.91, 140.70, 140.20, 139.90, 139.76, 139.70, 139.65, 131.71, 130.67, 130.32, 130.24, 130.05, 129.80, 129.63, 129.47, 128.68, 128.15, 123.95, 123.78, 120.16, 118.92, 115.05; ESI-MS $[\mathbf{2a}(PF_6)_4]^{4+}$ 918.57, $[\mathbf{2a}(PF_6)_5]^{3+}$ 1272.64. Found: C, 47.11; H, 7.03; N, 10.35%. Calc. for $C_{168}H_{120}Cu_8F_{48}N_{32}P_8{\cdot}2H_2O$: C, 47.02; H, 2.91; N, 10.45%.

General Synthetic Procedure for 2a·BF_4 and 3a·BF_4. To a Schlenk flask was added [1,1′:4′,1″-terphenyl]-3,3″,5,5″-tetraamine **A** (4 equiv), suitable 2-pyridinecarboxaldehyde (16 equiv), $Cu(CH_3CN)_4BF_4$ (8 equiv) and acetonitrile. The solution was degassed by three evacuation/nitrogen fill cycles and stirred at room temperature for 24 h. The product was purified by recrystallization: diethyl ether was diffused into an acetonitrile solution of the complex. The desired complex was isolated by filtration as a black solid.

2a·BF_4: ^{1}H NMR (CD_3CN, 500 MHz) 9.778 (8H, s, imine *H*), 9.483 (8H, s, imine *H*), 8.500 (4H, s, Ph-*H*), 8.319 (8H, d, *J* 4.8, py-*H*), 8.225 (16H, py-*H*), 8.066 (24H, py-*H*), 7.946 (4H, s, Ph-*H*), 7.565 (16H, py-*H*), 7.175 (8H, s, Ph-*H*), 7.056 (8H, d, *J* 8.0, Ph-*H*), 6.701 (8H, d, *J* 8.0, Ph-*H*; ^{13}C {^{1}H} NMR (CD_3CN, 125 MHz) 162.34, 158.96, 151.59, 151.54, 150.19, 149.82, 149.76, 147.72, 145.08, 143.94, 140.12, 139.93, 139.60, 139.58, 130.29, 130.05, 129.97, 129.91, 129.67, 127.99, 127.95, 124.26, 120.13, 106.75; MALDI-MS $[\mathbf{2a}(BF_4)_7]^+$ 3701.4. Found: C, 49.70; H, 3.17; N, 10.84%. Calc. for $C_{168}H_{120}B_8Cu_8F_{32}N_{32}{\cdot}14H_2O$: C, 49.92; H, 3.69; N, 11.09%.

3a·BF_4: ^{1}H NMR (CD_3CN, 500 MHz) 9.783 (8H, s, imine *H*), 9.464 (8H, s, imine *H*), 8.599 (4H, s, Ph-*H*), 8.260 (8H, d, *J* 7.5, py-*H*), 8.136 (8H, d, py-*H*), 8.113 (8H, s, Ph-*H*), 7.991 (8H, t, *J* 7.5, py-*H*), 7.980 (8H, t, *J* 7.5, py-*H*), 7.822 (8H, d, *J* 7.5, py-*H*), 7.756 (8H, d, *J* 7.5, py-*H*), 7.322 (8H, s, Ph-*H*), 7.172 (8H, d, br, Ph-*H*), 6.784 (8H, d, *J* 7.0, Ph-*H*); ^{13}C {^{1}H} NMR (CD_3CN, 125 MHz) 162.05, 157.83, 152.80, 152.75, 149.77, 146.69, 145.38, 144.11 142.84, 142.69, 142.52, 141.98, 139.90, 139.29, 134.15, 134.08, 129.64, 129.38, 129.07, 127.95, 123.72, 120.38, 106.47; MALDI-MS $[\mathbf{3a}(BF_4)_7]^+$ 4964.1. Found: C, 39.15; H, 2.22; N, 8.58%. Calc. for $C_{168}H_{104}B_8Br_{16}Cu_8F_{32}N_{32}{\cdot}6H_2O$: C, 39.10; H, 2.27; N, 8.69%.

1b·PF_6. To a Schlenk tube was added **B**, [1,1′:4′,1″:4″,1‴-quaterphenyl]-3,3‴,5,5‴-tetraamine (30 mg, 0.08 mmol, 4 equiv), 6-methyl-2-pyridinecarboxaldehyde (39.7 mg, 0.32 mmol, 16 equiv), $Cu(CH_3CN)_4PF_6$ (61 mg, 0.16 mmol, 8 equiv) and acetonitrile (10 mL). The solution was degassed by three evacuation/nitrogen fill cycles and stirred at room temperature for 12 h. A dark pink solution resulted. The product was purified by recrystallization: diisopropyl ether was diffused into an acetonitrile solution of the complex. The desired product **1b**·PF_6 was isolated by filtration as a black solid (55 mg, 56%): ^{1}H NMR (CD_3CN, 500 MHz) the solution is a mixture of two isomers, D_4:D_{2d} = 13:87%, as shown in Figure S21 (Supporting Information), 10.30 (8H, s, br, imine *H*), 9.39 (8H, s, imine *H*), 9.17 (8H, s, imine *H*), 8.55 (4H, br, Ph-*H*), 8.58 (8H, t, *J* 7.75, py-*H*), 8.53 (4H, br, Ph-*H*), 8.10 (s, Ar-*H*), 8.06 (m, br, Ar-*H*), 7.99 (m, Ar-*H*), 7.92 (m, Ar-*H*), 7.83 (m, br, Ar-*H*), 7.77 (8H, d, *J* 7.40, Ph-*H*), 7.71 (8H, d, *J* 7.85, Ph-*H*), 7.67 (8H, s, Ar-*H*), 7.61 (8H, d, *J* 6.75, Ph-*H*), 7.57 (8H, d, *J* 6.75, Ph-*H*), 7.48 (8H, d, *J* 7.05, py-*H*), 7.38 (8H, d, *J* 7.45, py-*H*), 7.27 (8H, d, *J* 7.35, Ph-*H*), 7.21 (8H, s, Ph-*H*), 7.13 (8H, d, *J* 7.00, Ph-*H*), 6.90 (8H, s, Ph-*H*), 6.66 (8H, d, *J* 7.05, Ph-*H*), 6.52 (8H, d, *J* 7.25, Ph-*H*), 2.55 (24H, s, CH_3), 2.47 (24H, s, CH_3), 2.08 (24H, s, CH_3), 1.72 (24H, s, CH_3); ^{13}C {^{1}H} NMR (CD_3CN, 125 MHz) 163.19, 162.58, 162.36, 161.70, 160.96, 160.53, 159.53, 159.42, 158.68, 151.48, 150.91, 150.71, 150.29, 150.22, 150.03, 149.95, 147.85, 144.70, 144.57, 143.91, 140.49, 140.24, 139.69, 139.49, 139.46, 139.41, 139.35, 138.35, 131.59, 130.37, 130.09, 129.43, 129.37, 128.67, 128.51, 128.40, 128.27, 127.71, 127.60, 127.33, 127.26, 127.10, 124.36, 123.66, 119.76, 119.12, 114.88, 26.41, 25.99, 24.92, 23.88; ESI-MS $[\mathbf{1b}]^{8+}$ 452.96, $[\mathbf{1b}(PF_6)]^{7+}$ 538.53, $[\mathbf{1b}(PF_4)_2]^{6+}$ 652.22, $[\mathbf{1b}(PF_6)_3]^{5+}$ 811.71, $[\mathbf{1b}(PF_6)_4]^{4+}$ 1051.12. Found: C, 52.91; H, 3.87; N, 9.50%. Calc. for $C_{208}H_{168}Cu_8F_{48}N_{32}P_8{\cdot}2C_6H_4O$ (diisopropyl ether): C, 52.97; H, 3.69; N, 8.99%.

1b·BF_4. To a NMR tube was added **B**, [1,1′:4′,1″:4″,1‴-quaterphenyl]-3,3‴,5,5‴-tetraamine (8 mg, 0.02 mmol, 4 equiv), 6-methyl-2-pyridinecarboxaldehyde (10.5 mg, 0.08 mmol, 16 equiv), $Cu(CH_3CN)_4BF_4$ (13.7 mg, 0.04 mmol, 8 equiv) and acetonitrile (1 mL). The resulting dark pink solution was kept at 50 °C for 12 h. Diethyl ether was added into the reaction mixture; the resulting mixture was centrifuged, and the solvent was decanted. The solid was dried under a high vacuum to give the desired product **1b**·BF_4 as

dx.doi.org/10.1021/ja412964r | J. Am. Chem. Soc. 2014, 136, 3972−3980

a dark pink solid (22.2 mg, 94%). **1b**-D_4:**1b**-D_{2d} = 99:1%, calculated from the integration of CH_3 signals in the ^{1}H NMR spectrum (i.e., peaks at 2.55, 2.48 ppm). NMR data for D_{2d} isomer reported here: ^{1}H NMR (CD_3CN, 400 MHz) 9.76 (8H, s, imine *H*), 9.39 (8H, s, imine *H*), 8.46 (4H, s, Ph-*H*), 8.09−8.03 (20H, Ar-*H*), 7.99−7.92 (24H, Ar-*H*), 7.61−7.54 (16H, Ar-*H*), 7.46 (8H, s, Ph-*H*), 7.44 (8H, s, Ph-*H*), 7.23 (8H, d, *J* 8.08, Ph-*H*), 7.15 (8H, s, Ph-*H*), 6.49 (8H, d, *J* 8.08, Ph-*H*), 2.13 (24H, s, CH_3), 1.70 (24H, s, CH_3); ^{13}C {^{1}H} NMR (CD_3CN, 125 MHz) 162.54, 159.47, 159.26, 158.98, 150.85, 150.85, 149.81, 147.61, 144.65, 144.24, 140.22, 139.65, 139.36, 139.21, 139.09, 138.44, 130.06, 129.72, 129.34, 128.67, 128.31, 128.11, 127.81, 127.58, 127.31, 127.25, 124.23, 119.65, 106.89, 25.01, 23.74; ESI-MS [**1b**]$^{8+}$ 439.92, [**1b**(BF_4)]$^{7+}$ 515.24, [**1b**$(BF_4)_2$]$^{6+}$ 615.43, [**1b**$(BF_4)_3$]$^{5+}$ 755.93, [**1b**$(BF_4)_4$]$^{4+}$ 966.81, [**1b**$(BF_4)_5$]$^{3+}$ 1317.78. Found: C, 55.84; H, 3.96; N, 10.00%. Calc. for $C_{208}H_{168}Cu_8F_{32}N_{32}B_8\cdot 12H_2O$: C, 55.09; H, 4.27; N, 9.88%.

1c·PF_6. To a Schlenk tube was added **C**, 5,5′-(naphthalene-2,6-diyl)bis(benzene-1,3-diamine) (20 mg, 0.06 mmol, 4 equiv), 6-methyl-2-pyridinecarboxaldehyde (28.5 mg, 0.23 mmol, 16 equiv), Cu$(CH_3CN)_4PF_6$ (44 mg, 0.12 mmol, 8 equiv) and acetonitrile (5 mL). The solution was degassed by three evacuation/nitrogen fill cycles and stirred at room temperature for 12 h. A dark pink solution resulted. The product was precipitated by adding diethyl ether into the reaction mixture and was isolated by filtration as dark pink solid (20 mg, 29%). **1c**-D_2:**1c**-D_4 = 96:4%, calculated from the integration of CH_3 signals in the ^{1}H NMR spectrum (i.e., peaks at 2.54, 2.46 ppm). NMR data for D_2 isomer reported here: ^{1}H NMR (CD_3CN, 400 MHz) 9.84 (8H, br, imine *H*), 9.40 (8H, s, imine *H*), 8.54 (4H, br, Ar-*H*), 8.22 (4H, br, Ar-*H*), 8.12 (4H, s, Ph-*H*), 8.00−7.91 (36H, Ar-*H*), 7.86 (4H, d, *J* 8.32, naph-*H*), 7.73 (4H, d, *J* 8.36, naph-*H*), 7.48−7.37 (28H, Ar-*H*), 7.00 (4H, s, naph-*H*), 6.68 (4H, d, *J* 8.68, naph-*H*), 6.47 (4H, d, *J* 8.28, naph-*H*), 2.13 (24H, s, CH_3, overlapping with H_2O signals), 1.73 (24H, s, CH_3); ^{13}C {^{1}H} NMR (CD_3CN, 125 MHz) 162.46, 160.04, 159.55, 159.01, 151.15, 151.01, 149.93, 147.99, 145.10, 143.62, 140.07, 139.79, 137.73, 137.09, 133.61, 133.48, 130.26, 130.20, 129.95, 129.74, 128.23, 128.07, 127.65, 127.08, 126.33, 125.33, 124.53, 119.88, 107.81, 26.39, 25.93, 24.98, 23.79; ESI-MS [**1c**]$^{8+}$ 439.95, [**1c**(PF_6)]$^{7+}$ 523.48, [**1c**$(PF_6)_2$]$^{6+}$ 634.87, [**1c**$(PF_6)_3$]$^{5+}$ 790.91, [**1c**$(PF_6)_4$]$^{4+}$ 1024.77, [**1c**$(PF_6)_5$]$^{3+}$ 1414.65. Found: C, 50.29; H, 3.45; N, 9.20%. Calc. for $C_{200}H_{160}Cu_8F_{48}N_{32}P_8\cdot 5H_2O$: C, 50.36; H, 3.59; N, 9.40%.

1c·BF_4. To a NMR tube was added **C**, 5,5′-(naphthalene-2,6-diyl)bis(benzene-1,3-diamine) (6 mg, 17.6 μmol, 4 equiv), 6-methyl-2-pyridinecarboxaldehyde (8.5 mg, 70.5 μmol, 16 equiv), Cu$(CH_3CN)_4BF_4$ (11 mg, 35.2 μmol, 8 equiv) and acetonitrile (1 mL). The resulting dark pink solution was kept at 50 °C for 12 h. Diethyl ether was added into the reaction mixture; the resulting mixture was centrifuged, and the solvent was decanted. The solid was dried under a high vacuum to give the desired product **1c**·BF_4 as a dark pink solid (14.4 mg, 77%): ^{1}H NMR (CD_3CN, 400 MHz) 9.78 (8H, s, imine *H*), 9.43 (8H, s, imine *H*), 8.51 (4H, s, Ph-*H*), 8.13−8.09 (12H, py-*H*), 8.00−7.93 (32H, Ar-*H*), 7.87 (4H, d, *J* 8.36, naph-*H*), 7.75 (4H, d, *J* 8.28, naph-*H*), 7.47 (8H, s, Ph-*H*), 7.45 (8H, s, Ph-*H*), 7.41 (4H, s, naph-*H*), 7.35 (8H, s, naph-*H*), 6.66 (4H, d, *J* 8.36, naph-*H*), 6.48 (4H, d, *J* 8.36, naph-*H*), 2.14 (24H, s, CH_3), 1.72 (24H, s, CH_3); ^{13}C {^{1}H} NMR (CD_3CN, 125 MHz) 162.58, 159.58, 159.49, 159.08, 150.97, 150.83, 149.86, 147.88, 145.00, 143.68, 140.27, 139.74, 137.73, 136.90, 133.54 133.42, 130.25, 130.12, 129.84, 127.90, 127.80, 127.61, 127.02, 126.95, 126.35, 125.23, 124.41, 119.83, 107.25, 24.98, 23.70; ESI-MS [**1c**]$^{8+}$ 452.91, [**1c**(BF_4)]$^{7+}$ 530.29, [**1c**$(BF_4)_2$]$^{6+}$ 632.81, [**1c**$(BF_4)_3$]$^{5+}$ 776.73, [**1c**$(BF_4)_4$]$^{4+}$ 992.65, [**1c**$(BF_4)_5$]$^{3+}$ 1352.19. Found: C, 53.84; H, 3.98; N, 10.09%. Calc. for $C_{200}H_{160}Cu_8F_{32}N_{32}B_8\cdot 14H_2O$: C, 53.78; H, 4.24; N, 10.03%.

[Au(Au(CN)$_2$)$_2$ ⊂ 1a]·BF_4. [Cu(Au(CN)$_2$)$_2$ ⊂ **1a**]·BF_4 (6.6 mg, 1.5 μmol, 1 equiv), Au(tmbn)$_2$$SbF_6$ (1.4 mg, 1.7 μmol, 1.1 equiv) and MeCN (0.35 mL) were mixed in a NMR tube. The tube was rotated on a turner at room temperature for 12 h. Diethyl ether was then added, and the product was collected by filtration as a plum-colored solid (4 mg, 59%). ^{1}H NMR revealed the presence of [Au(Au(CN)$_2$)$_2$ ⊂ **1a**]·BF_4, [Cu(Au(CN)$_2$)$_2$ ⊂ **1a**]·BF_4 and **1a**·BF_4 in a ratio of 87:9:4%. Further addition of Au(tmbn)$_2$$SbF_6$ did not increase the amount of the desired product but produced more **1a**. Characterization data for [Au(Au(CN)$_2$)$_2$ ⊂ **1a**]·BF_4: ^{1}H NMR (CD_3CN, 400 MHz) 9.44−9.38 (8H, imine *H*), 8.44−8.39 (8H, py-*H*), 8.05−7.79 (48H, Ar-*H*), 7.62 (8H, br, Ar-*H*), 7.30−7.13 (16H, Ar-*H*), 7.04−6.95 (16H, Ar-*H*), 2.50 (24H, s, CH_3), 2.39 (24H, br, CH_3); ^{13}C {^{1}H} NMR (CD_3CN, 125 MHz) peaks split from one carbon signal are grouped in parentheses (161.48, 161.41, 161.34), 160.53, 160.08, 159.28, 151.53, (151.03, 150.98), 150.54, (149.59, 149.56, 149.52), (149.14, 149.10), (143.48, 143.19, 143.02), 139.61, 139.45, 138.86, 138.60, 138.43, 131.06, 130.62, 129.95, (129.15, 129.06, 128.90), 128.05, 127.53, (124.65, 124.42, 124.29), 117.74, 114.94, 26.19, 25.88; guest signals 152.0 (d, *J* 10.0), 152.5 (d, *J* 13.75), 152.8 (d, *J* 12.8), 149.24, 135.86, 135.44, 134.77; ESI-MS [Au(Au(CN)$_2$)$_2$ ⊂ **1a** (BF_4)]$^{6+}$ 683.52, [Au(Au(CN)$_2$)$_2$ ⊂ **1a** $(BF_4)_2$]$^{5+}$ 837.51, [Au(Au(CN)$_2$)$_2$ ⊂ **1a** $(BF_4)_3$]$^{4+}$ 1068.79, [Au(Au(CN)$_2$)$_2$ ⊂ **1a** $(BF_4)_4$]$^{3+}$ 1453.69.

[Ag(Au(CN)$_2$)$_2$ ⊂ 1a]·PF_6. **1a**·PF_6 (30 mg, 7 μmol, 1 equiv), $KAu(CN)_2$ (4.1 mg, 14 μmol, 2 equiv), Cu$(NCMe)_4PF_6$ (2.6 mg, 7 μmol, 1 equiv) and MeCN (5 mL) were mixed in a vial. The reaction mixture was stirred at room temperature for 12 h. Diethyl ether was then added, and the desired complex [Ag(Au(CN)$_2$)$_2$ ⊂ **1a**]·PF_6 was collected by filtration as a plum colored solid (38 mg, 70%): ^{1}H NMR (CD_3CN, 400 MHz) 9.32 (8H, s, imine *H*), 8.39 (8H, t, *J* 7.76, Ph-*H*), 8.06−8.00 (24H, Ar-*H*), 7.83 (8H, d, *J* 7.96, py-*H*), 7.80 (8H, d, *J* 7.60, py-*H*), 7.74 (8H, s, Ph-*H*), 7.65 (8H, dd, *J* 6.72, 2.16, py-*H*), 7.11 (16H, s, Ph-*H*), 6.98 (16H, d, *J* 1.12, Ph-*H*), 2.49 (24H, s, CH_3), 2.39 (24H, s, CH_3); ^{13}C {^{1}H} NMR (CD_3CN, 125 MHz) 161.40, 160.93, 160.09, 159.30, 150.96, 150.53, 149.66, 149.37, 143.48, 139.56, 130.60, 130.04, 128.79, 128.15, 127.51, 124.83, 115.15, 26.21, 25.77; ESI-MS [Ag(Au(CN)$_2$)$_2$ ⊂ **1a**]$^{7+}$ 560.72, [Ag(Au(CN)$_2$)$_2$ ⊂ **1a** (PF_6)]$^{6+}$ 678.22, [Ag(Au(CN)$_2$)$_2$ ⊂ **1a** $(PF_6)_2$]$^{5+}$ 842.87, [Ag(Au(CN)$_2$)$_2$ ⊂ **1a** $(PF_6)_3$]$^{4+}$ 1090.03, [Ag(Au(CN)$_2$)$_2$ ⊂ **1a** $(PF_6)_4$]$^{3+}$ 1501.61; Found: C, 43.56; H, 3.08; N, 9.66%. Calc. for $C_{188}H_{152}AgAu_2Cu_8F_{42}N_{36}P_7\cdot 13H_2O$: C, 43.64; H, 3.47; N, 9.74%.

[Cu(Au(CN)$_2$)$_2$ ⊂ 1c]·PF_6. **1c**·PF_6 (50 mg, 10.7 mmol, 1 equiv), $KAu(CN)_2$ (6.1 mg, 21.4 mmol, 2 equiv), Cu$(NCMe)_4PF_6$ (4.0 mg, 10,7 mmol, 1 equiv) and MeCN (5 mL) were mixed in a Schlenk flask. The reaction mixture was stirred at room temperature for 5 h. Diethyl ether was added into the reaction mixture; the resulting mixture was centrifuged, and the solvent was decanted. The solid was dried under a high vacuum to give the desired product [Cu(Au(CN)$_2$)$_2$ ⊂ **1c**]·PF_6 as a dark pinkish-red solid (30 mg, 86%): ^{1}H NMR (CD_3CN, 400 MHz) 9.27 (8H, s, imine-*H*), 8.59 (8H, t, *J* 7.48, py-*H*), 8.06 (8H, t, *J* 7.68, py-*H*), 8.04 (8H, s, imine-*H*), 7.96 (8H, d, *J* 6.40, py-*H*), 7.94 (8H, d, *J* 7.20, py-*H*), 7.87 (8H, d, *J* 7.88, py-*H*), 7.69 (8H, d, *J* 8.04, py-*H*), 7.67 (8H, s, Ph-*H*), 7.45 (8H, s, Ph-*H*), 7.04 (8H, s, naph-*H*), 6.90 (16H, s, naph-*H*), 6.80 (8H, s, Ph-*H*), 2.50 (24H, s, CH_3), 2.49 (24H, s, CH_3); ^{13}C {^{1}H} NMR (CD_3CN, 125 MHz) 161.97, 161.28, 160.47, 159.32, (Guest signals 153.29, 152.91, d, J_{C-Au-C} 47.8, 151.42, 151.04, d, J_{C-Au-C} 47.8) 150.95, 150.86, 150.85, 150.08, 149.53, 144.06, 140.27, 139.55, 137.39, 133.41, 130.94, 130.10, 129.98, 127.74, 127.53, 127.49, 126.85, 123.88, 118.25, 115.38, 26.48, 25.73; ESI-MS [Cu(Au(CN)$_2$)$_2$ ⊂ L_4Cu_8]$^{7+}$ 583.05, [Cu(Au(CN)$_2$)$_2$ ⊂ **1c**(PF_6)]$^{6+}$ 704.37, [Cu(Au(CN)$_2$)$_2$ ⊂ **1c**$(PF_6)_2$]$^{5+}$ 874.26, [Cu(Au(CN)$_2$)$_2$ ⊂ **1c**$(PF_6)_3$]$^{4+}$ 1129.01, [Cu(Au(CN)$_2$)$_2$ ⊂ **1c**$(PF_6)_4$]$^{3+}$ 1553.50. Found: C, 45.50; H, 3.15; N, 9.22%. Calc. for $C_{204}H_{160}Cu_9Au_2F_{42}N_{36}P_7\cdot 15H_2O$: C, 45.66; H, 3.57; N, 9.40%.

[Ag(Au(CN)$_2$)$_2$ ⊂ 1c]·PF_6. To [Cu(Au(CN)$_2$)$_2$ ⊂ **1c**-D_4]·PF_6 (5 mg, 0.98 μmol, 1 equiv) was added a stock solution of $AgPF_6$ (0.3 mg, 1.2 μmol, 1.2 equiv of stock solution prepared using 37 mg $AgPF_6$ and 0.5 mL CD_3CN). The resulting solution was heated at 40 °C for 4 h. Diethyl ether was added into the reaction mixture, which was centrifuged, and then the solvent was decanted. The solid was dried under a high vacuum to give the desired product [Ag(Au(CN)$_2$)$_2$ ⊂ **1c**]·PF_6 as a dark pinkish-red solid (5.3 mg, 96%): ^{1}H NMR (CD_3CN, 500 MHz) 9.26 (8H, s, imine *H*), 8.56 (8H, t, *J* 7.77, py-*H*), 8.06 (16H, imine-*H* and py-*H*), 7.96 (8H, d, *J* 7.60, py-*H*), 7.94 (8H, d, *J* 7.60, py-*H*), 7.87 (8H, d, *J* 7.90, py-*H*), 7.69 (8H, d, *J* 7.55, py-*H*), 7.65 (8H, s, Ph-*H*), 7.46 (8H, s, naph-*H*), 7.04 (8H, s, Ph-*H*), 6.90−6.87 (16H, m, naph-*H*), 6.82 (8H, s, Ph-*H*), 2.50 (24H, s, CH_3), 2.48 (24H, s, CH_3); ^{13}C {^{1}H} NMR (CD_3CN, 125 MHz) 162.04, 161.32, 160.40, 159.36, 150.97, 150.83, 150.05, 149.57, 144.09, 140.19, 139.57,

dx.doi.org/10.1021/ja412964r | J. Am. Chem. Soc. 2014, 136, 3972−3980

137.59, 133.40 130.91, 130.13, 129.51, 127.96, 127.77, 127.54, 127.03, 124.06, 115.37, 26.47, 25.75 (Guest signals 153.1, dd, $J_{C-Au-C,\ C-N-Ag}$ 47.1, 26.0, and 152.3, d, J_{C-Au-C} 46.8); ESI-MS $[Ag(Au(CN)_2)_2 \subset \mathbf{1c}]^{7+}$ 589.40, $[Ag(Au(CN)_2)_2 \subset \mathbf{1c}\ (PF_6)]^{6+}$ 711.55, $[Ag(Au(CN)_2)_2 \subset \mathbf{1c}(PF_6)_2]^{5+}$ 883.05, $[Ag(Au(CN)_2)_2 \subset \mathbf{1c}(PF_6)_3]^{4+}$ 1140.01, $[Ag(Au(CN)_2)_2 \subset \mathbf{1c}(PF_6)_4]^{3+}$ 1568.57. Found: C, 46.35; H, 3.07; N, 9.87%. Calc. for $C_{204}H_{160}AgCu_8Au_2F_{42}N_{36}P_7{\cdot}7H_2O$: C, 46.52; H, 3.33; N, 9.57%.

$[Au(Au(CN)_2)_2 \subset \mathbf{1c}]{\cdot}PF_6$. To $[Cu(Au(CN)_2)_2 \subset \mathbf{1c}\text{-}D_4]{\cdot}PF_6$ (6.2 mg, 1.2 μmol, 1 equiv) in CD_3CN (0.35 mL) in a j-young tube was added $Au(tmbn)_2SbF_6$ (1.2 mg, 1.5 μmol, 1.2 equiv). The tube was rotated on a turner at room temperature for 12 h. ^{1}H NMR showed 50% of the starting material was converted to $[Au(Au(CN)_2)_2 \subset \mathbf{1c}]{\cdot}PF_6$. Further addition of $Au(tmbn)_2SbF_6$ did not increase the amount of the desired product but converted left over $[Cu(Au(CN)_2)_2 \subset \mathbf{1c}]{\cdot}PF_6$ into $\mathbf{1c}$-D_2; ESI-MS $[Au(Au(CN)_2)_2 \subset \mathbf{1c}]^{7+}$ 602.06, $[Au(Au(CN)_2)_2 \subset \mathbf{1c}(PF_6)]^{6+}$ 726.60, $[Ag(Au(CN)_2)_2 \subset \mathbf{1c}(PF_6)_2]^{5+}$ 900.87, $[Ag(Au(CN)_2)_2 \subset \mathbf{1c}(PF_6)_3]^{4+}$ 1162.46, $[Ag(Au(CN)_2)_2 \subset \mathbf{1c}\ (PF_6)_4]^{3+}$ 1598.41.

4·BF_4. To a NMR tube were added [1,1′:4′,1″-terphenyl]-3,3″,5,5″-tetraamine **A** (1.5 mg, 5.2 μmol, 4 equiv), 6-methyl-2-pyridinecarboxaldehyde (2.5 mg, 20.7 μmol, 16 equiv), and acetonitrile (0.5 mL). The resulting mixture was heated at 50 °C overnight before $AgBF_4$ (2.0 mg, 10.3 μmol, 8 equiv) was added. The tube was turned at room temperature overnight. A bright yellow solution resulted. The product was purified by recrystallization: diethyl ether was diffused into an acetonitrile solution of the complex. The desired product **4**·BF_4 was isolated by filtration as yellow crystals (4.4 mg, 78%): ^{1}H NMR (CD_3CN, 500 MHz) 9.45 (8H, d, J_{Ag-H} 5.9, imine *H*), 9.33 (8H, d, J_{Ag-H} 7.8, imine *H*), 8.33 (4H, t, Ph-*H*), 8.06 (4H, t, *J* 1.75, Ph-*H*), 8.05−8.03 (16H, d, *J* 4.7, py-*H*), 7.96 (8H, s, Ph-*H*), 7.93 (8H, t, *J* 7.7, py-*H*), 7.87 (8H, d, *J* 7.6, py-*H*), 7.54−7.51 (16H, py-*H*), 7.27−7.26 (16H, Ph-*H*), 6.66 (8H, d, *J* 7.9, Ph-*H*), 2.51 (24H, CH_3), 2.07 (24H, CH_3); ^{13}C {^{1}H} NMR (CD_3CN, 125 MHz) 163.71, 160.76, 160.30, 159.63, 150.10, 149.54, 149.21, 147.98, 144.43, 143.70, 141.22, 140.54, 140.27, 139.84, 130.01, 129.54, 129.17, 128.97, 128.90, 128.81, 128.67, 128.13, 125.59, 118.81, 27.18, 25.58; MALDI-MS using DCTB (2-[(2*E*)-3-(4-tert-butylphenyl)-2-methylprop-2-enylidene]malononitrile) matrix observed 4280.6, calc. for $[L_4Cu_8(BF_4)_7]^+$ 4281.94. Found: C, 49.35; H, 3.43; N, 9.51%. Calc. for $C_{184}H_{152}B_8Ag_8F_{32}N_{32}{\cdot}5H_2O$: C, 49.56; H, 3.66; N, 10.05%.

Transmetalation. A stock solution was prepared using 18-crown-6 (6.2 mg, 23.4 μmol, 1.01 equiv), $KAg(CN)_2$ (4.6 mg, 23.1 μmol, 1 equiv) and CD_3CN (0.35 mL). To **1a**·PF_6 (4 mg, 0.9 μmol, 1 equiv) in CD_3CN (0.4 mL) in a NMR tube were added $KAg(CN)_2$ (0.37 mg, 1.8 μmol, 2 equiv, 28 μL stock solution) and $Au(tmbn)_2SbF_6$ (0.77 mg, 0.9 μmol, 1 equiv). The tube was rotated on a turner at room temperature for 12 h. ^{1}H NMR and ESI-MS showed the formation of $[Ag(Au(CN)_2)_2 \subset \mathbf{1a}\text{-}D_4]{\cdot}PF_6$.

■ ASSOCIATED CONTENT

Supporting Information

Synthesis and characterization for tetraamine **B** and **C**, NMR spectra for **1a**·PF_6, **2a**·BF_4, **2a**·PF_6, **3a**·BF_4, **1b**·BF_4, **1b**·PF_6, **1c**·BF_4, **1c**·PF_6, **4**·BF_4, $[Au(Au(CN)_2)_2 \subset \mathbf{1a}]{\cdot}BF_4$, $[Ag(Au(CN)_2)_2 \subset \mathbf{1a}]{\cdot}PF_6$, $[Cu(Au(CN)_2)_2 \subset \mathbf{1c}]{\cdot}PF_6$, $[Ag(Au(CN)_2)_2 \subset \mathbf{1c}]{\cdot}PF_6$, and $[Au(Au(CN)_2)_2 \subset \mathbf{1c}]{\cdot}PF_6$, kinetic study of isomerization for **1b**·BF_4, calculation of binding constants for $Au(Au(CN)_2)_2$, and crystallographic data (CIF). Crystallographic data has been deposited with the CCDC (numbers 846046, 955699, and 905144−905149). This material is available free of charge via the Internet at http://pubs.acs.org.

■ AUTHOR INFORMATION

Corresponding Author

jrn34@cam.ac.uk; cramer@umn.edu; gagliard@umn.edu

Present Addresses

[§]Clarendon Laboratory, Department of Physics, University of Oxford, Oxford, OX1 3PU, U.K.

[‖]School of Chemistry and Molecular Biosciences, The University of Queensland, Brisbane St Lucia, QLD, Australia, 4072.

Notes

The authors declare no competing financial interest.

■ ACKNOWLEDGMENTS

This work was supported by the U.K. Engineering and Physical Sciences Research Council (EPSRC), the US National Science Foundation (NSF) and the Marie Curie IIF Scheme of the 7th EU Framework Program. We thank the EPSRC Mass Spectrometry Service at Swansea for MALDI-TOF experiments, Diamond Light Source (U.K.) for synchrotron beamtime on I19 (MT7114 and MT7569), and the EPSRC National Crystallography Service at the University of Southampton for the collection of crystallographic data. We thank Ana M. Castilla for the preparation of $Au(tmbn)_2SbF_6$ and Emily V. Dry for the preparation of $Cu(CH_3CN)_4BF_4$.

■ REFERENCES

(1) Chakrabarty, R.; Mukherjee, P. S.; Stang, P. J. *Chem. Rev.* **2011**, *111*, 6810−6918.
(2) Ward, M. D. *Chem. Commun.* **2009**, 4487−4499.
(3) Fujita, M.; Tominaga, M.; Hori, A.; Therrien, B. *Acc. Chem. Res.* **2005**, *38*, 369−378.
(4) Dalgarno, S. J.; Power, N. P.; Atwood, J. L. *Coord. Chem. Rev.* **2008**, *252*, 825−841.
(5) Tranchemontagne, D. J.; Ni, Z.; O'Keeffe, M.; Yaghi, O. M. *Angew. Chem., Int. Ed.* **2008**, *47*, 5136−5147.
(6) Saalfrank, R. W.; Maid, H.; Scheurer, A. *Angew. Chem., Int. Ed.* **2008**, *47*, 8794−8824.
(7) Young, N. J.; Hay, B. P. *Chem. Commun.* **2013**, *49*, 1354−1379.
(8) Yoshizawa, M.; Klosterman, J. K.; Fujita, M. *Angew. Chem., Int. Ed.* **2009**, *48*, 3418−3438.
(9) Yoshizawa, M.; Tamura, M.; Fujita, M. *Science* **2006**, *312*, 251−254.
(10) Pluth, M. D.; Bergman, R. G.; Raymond, K. N. *Science* **2007**, *316*, 85−88.
(11) Hastings, C. J.; Fiedler, D.; Bergman, R. G.; Raymond, K. N. *J. Am. Chem. Soc.* **2008**, *130*, 10977−10983.
(12) Kuil, M.; Soltner, T.; Van Leeuwen, P. W. N. M.; Reek, J. N. H. *J. Am. Chem. Soc.* **2006**, *128*, 11344−11345.
(13) Otte, M.; Kuijpers, P. F.; Troeppner, O.; Ivanović-Burmazović, I.; Reek, J. N. H.; de Bruin, B. *Chem.—Eur. J.* **2013**, *19*, 10170−10178.
(14) Wang, Z. J.; Clary, K. N.; Bergman, R. G.; Raymond, K. N.; Toste, F. D. *Nat. Chem.* **2013**, *5*, 100−103.
(15) Gunnlaugsson, T.; Glynn, M.; Tocci, G. M.; Kruger, P. E.; Pfeffer, F. M. *Coord. Chem. Rev.* **2006**, *250*, 3094−3117.
(16) Kondo, K.; Suzuki, A.; Akita, M.; Yoshizawa, M. *Angew. Chem., Int. Ed.* **2013**, *52*, 2308−2312.
(17) Li, S.-S.; Northrop, B. H.; Yuan, Q.-H.; Wan, L.-J.; Stang, P. J. *Acc. Chem. Res.* **2008**, *42*, 249−259.
(18) Sessler, J. L.; Camiolo, S.; Gale, P. A. *Coord. Chem. Rev.* **2003**, *240*, 17−55.
(19) Smith, D. K.; Diederich, F. *Top. Curr. Chem.* **2000**, *210*, 183−227.
(20) Watt, M. M.; Zakharov, L. N.; Haley, M. M.; Johnson, D. W. *Angew. Chem., Int. Ed.* **2013**, *52*, 10275−10280.
(21) Dong, V. M.; Fiedler, D.; Carl, B.; Bergman, R. G.; Raymond, K. N. *J. Am. Chem. Soc.* **2006**, *128*, 14464−14465.
(22) Mal, P.; Breiner, B.; Rissanen, K.; Nitschke, J. R. *Science* **2009**, *324*, 1697−1699.

(23) Sawada, T.; Yoshizawa, M.; Sato, S.; Fujita, M. *Nat. Chem.* **2009**, *1*, 53−56.
(24) Yoshizawa, M.; Tamura, M.; Fujita, M. *Angew. Chem., Int. Ed.* **2007**, *46*, 3874−3876.
(25) Riddell, I. A.; Smulders, M. M. J.; Clegg, J. K.; Nitschke, J. R. *Chem. Commun.* **2011**, *47*, 457−459.
(26) Kishi, N.; Akita, M.; Kamiya, M.; Hayashi, S.; Hsu, H.-F.; Yoshizawa, M. *J. Am. Chem. Soc.* **2013**, *135*, 12976−12979.
(27) Berna, J.; Leigh, D. A.; Lubomska, M.; Mendoza, S. M.; Perez, E. M.; Rudolf, P.; Teobaldi, G.; Zerbetto, F. *Nat. Mater.* **2005**, *4*, 704−710.
(28) Sakai, N.; Matile, S. *Langmuir* **2013**, *29*, 9031−9040.
(29) Custelcean, R.; Bonnesen, P. V.; Duncan, N. C.; Zhang, X. H.; Watson, L. A.; Van Berkel, G.; Parson, W. B.; Hay, B. P. *J. Am. Chem. Soc.* **2012**, *134*, 8525−8534.
(30) Belowich, M. E.; Stoddart, J. F. *Chem. Soc. Rev.* **2012**, *41*, 2003−2024.
(31) Osowska, K.; Miljanić, O. Š. *Angew. Chem., Int. Ed.* **2011**, *50*, 8345−8349.
(32) Bunzen, H.; Nonappa; Kalenius, E.; Hietala, S.; Kolehmainen, E. *Chem.—Eur. J.* **2013**, *19*, 12978−12981.
(33) Campbell, V. E.; de Hatten, X.; Delsuc, N.; Kauffmann, B.; Huc, I.; Nitschke, J. R. *Chem.—Eur. J.* **2009**, *15*, 6138−6142.
(34) Dömer, J.; Slootweg, J. C.; Hupka, F.; Lammertsma, K.; Hahn, F. E. *Angew. Chem., Int. Ed.* **2010**, *49*, 6430−6433.
(35) Wu, Y.; Zhou, X.-P.; Yang, J.-R.; Li, D. *Chem. Commun.* **2013**, *49*, 3413−3415.
(36) Nitschke, J.; Ronson, T.; Zarra, S.; Black, S. P. *Chem. Commun.* **2012**, *49*, 2476−2490.
(37) Bilbeisi, R. A.; Clegg, J. K.; Elgrishi, N.; Hatten, X. d.; Devillard, M.; Breiner, B.; Mal, P.; Nitschke, J. R. *J. Am. Chem. Soc.* **2012**, *134*, 5110−5119.
(38) Ferguson, A.; Squire, M. A.; Siretanu, D.; Mitcov, D.; Mathoniere, C.; Clerac, R.; Kruger, P. E. *Chem. Commun.* **2013**, *49*, 1597−1599.
(39) Mal, P.; Schultz, D.; Beyeh, K.; Rissanen, K.; Nitschke, J. R. *Angew. Chem., Int. Ed.* **2008**, *47*, 8297−8301.
(40) Yi, S.; Brega, V.; Captain, B.; Kaifer, A. E. *Chem. Commun.* **2012**, *48*, 10295−10297.
(41) Chepelin, O.; Ujma, J.; Wu, X. H.; Slawin, A. M. Z.; Pitak, M. B.; Coles, S. J.; Michel, J.; Jones, A. C.; Barran, P. E.; Lusby, P. J. *J. Am. Chem. Soc.* **2012**, *134*, 19334−19337.
(42) Meng, W.; Breiner, B.; Rissanen, K.; Thoburn, J. D.; Clegg, J. K.; Nitschke, J. R. *Angew. Chem., Int. Ed.* **2011**, *50*, 3479−3483.
(43) Liu, Y.; Kravtsov, V.; Walsh, R. D.; Poddar, P.; Srikanth, H.; Eddaoudi, M. *Chem. Commun.* **2004**, 2806−2807.
(44) Stephenson, A.; Ward, M. D. *Dalton Trans.* **2011**, 10360−10369.
(45) Zhou, X.-P.; Liu, J.; Zhan, S.-Z.; Yang, J.-R.; Li, D.; Ng, K.-M.; Sun, R. W.-Y.; Che, C.-M. *J. Am. Chem. Soc.* **2012**, *134*, 8042−8045.
(46) Zhou, X. P.; Wu, Y.; Li, D. *J. Am. Chem. Soc.* **2013**, *135*, 16062−16065.
(47) Bilbeisi, R. A.; Ronson, T. K.; Nitschke, J. R. *Angew. Chem., Int. Ed.* **2013**, *52*, 9027−9030.
(48) Meng, W.; Ronson, T. K.; Clegg, J. K.; Nitschke, J. R. *Angew. Chem., Int. Ed.* **2013**, *52*, 1017−1021.
(49) Sham, K.-C.; Yiu, S.-M.; Kwong, H.-L. *Inorg. Chem.* **2013**, *52*, 5648−5650.
(50) Riddell, I. A.; Smulders, M. M. J.; Clegg, J. K.; Hristova, Y. R.; Breiner, B.; Thoburn, J. D.; Nitschke, J. R. *Nat. Chem.* **2012**, *4*, 751−756.
(51) Riddell, I. A.; Hristova, Y. R.; Clegg, J. K.; Wood, C. S.; Breiner, B.; Nitschke, J. R. *J. Am. Chem. Soc.* **2013**, *135*, 2723−2733.
(52) Meng, W.; Ronson, T. K.; Nitschke, J. R. *Proc. Natl. Acad. Sci. U. S. A.* **2013**, *110*, 10531−10535.
(53) Meng, W.; Clegg, J. K.; Nitschke, J. R. *Angew. Chem., Int. Ed.* **2012**, *51*, 1881−1884.
(54) Ustinov, A.; Weissman, H.; Shirman, E.; Pinkas, I.; Zuo, X.; Rybtchinski, B. *J. Am. Chem. Soc.* **2011**, *133*, 16201−16211.
(55) Han, M.; Michel, R.; He, B.; Chen, Y.-S.; Stalke, D.; John, M.; Clever, G. H. *Angew. Chem., Int. Ed.* **2013**, *52*, 1319−1323.
(56) Bong, D. T.; Clark, T. D.; Granja, J. R.; Ghadiri, M. R. *Angew. Chem., Int. Ed.* **2001**, *40*, 988−1011.
(57) Kimizuka, N.; Kawasaki, T.; Hirata, K.; Kunitake, T. *J. Am. Chem. Soc.* **1995**, *117*, 6360−6361.
(58) Matile, S.; Som, A.; Sorde, N. *Tetrahedron* **2004**, *60*, 6405−6435.
(59) Ajami, D.; Rebek, J. *Acc. Chem. Res.* **2013**, *46*, 990−999.
(60) Aoyagi, M.; Tashiro, S.; Tominaga, M.; Biradha, K.; Fujita, M. *Chem. Commun.* **2002**, 2036−2037.
(61) Tominaga, M.; Tashiro, S.; Aoyagi, M.; Fujita, M. *Chem. Commun.* **2002**, 2038−2039.
(62) Chifotides, H. T.; Giles, I. D.; Dunbar, K. R. *J. Am. Chem. Soc.* **2013**, *135*, 3039−3055.
(63) Glasson, C. R. K.; Meehan, G. V.; Motti, C. A.; Clegg, J. K.; Davies, M. S.; Lindoy, L. F. *Aust. J. Chem.* **2012**, *65*, 1371−1376.
(64) Coles, S. J.; Gale, P. A. *Chem. Sci.* **2012**, *3*, 683−689.
(65) Hibble, S. J.; Cheyne, S. M.; Hannon, A. C.; Eversfield, S. G. *Inorg. Chem.* **2002**, *41*, 1042−1044.
(66) Veldkamp, A.; Frenking, G. *Organometallics* **1993**, *12*, 4613−4622.
(67) Selig, W. S. *Microchem. J.* **1985**, *32*, 18−23.
(68) Ludlow, R. F.; Otto, S. *Chem. Soc. Rev.* **2008**, *37*, 101−108.
(69) Badjic, J. D.; Balzani, V.; Credi, A.; Silvi, S.; Stoddart, J. F. *Science* **2004**, *303*, 1845−1849.
(70) Hernandez, J. V.; Kay, E. R.; Leigh, D. A. *Science* **2004**, *306*, 1532−1537.
(71) Gianneschi, N. C.; Nguyen, S. T.; Mirkin, C. A. *J. Am. Chem. Soc.* **2005**, *127*, 1644−1645.
(72) Thordarson, P.; Bijsterveld, E. J. A.; Rowan, A. E.; Nolte, R. J. M. *Nature* **2003**, *424*, 915−918.
(73) Ray, D.; Foy, J. T.; Hughes, R. P.; Aprahamian, I. *Nat. Chem.* **2012**, *4*, 757−762.
(74) Hilson, G.; Monhemius, A. J. *J. Cleaner Prod.* **2006**, *14*, 1158−1167.
(75) Grimme, S.; Antony, J.; Ehrlich, S.; Krieg, H. *J. Chem. Phys.* **2010**, *132*, 154104−154119.
(76) Perdew, J. P.; Burke, K.; Ernzerhof, M. *Phys. Rev. Lett.* **1996**, *77*, 3865−3868.
(77) *ADF*; SCM, Theoretical Chemistry, Vrije Universiteit: Amsterdam, The Netherlands, 2013.
(78) Fonseca Guerra, C.; Snijders, J. G.; te Velde, G.; Baerends, E. J. *Theor. Chem. Acc.* **1998**, *99*, 391−403.
(79) te Velde, G.; Bickelhaupt, F. M.; Baerends, E. J.; Fonseca Guerra, C.; van Gisbergen, S. J. A.; Snijders, J. G.; Ziegler, T. *J. Comput. Chem.* **2001**, *22*, 931−967.
(80) van Lenthe, E.; Baerends, E. J. *J. Comput. Chem.* **2003**, *24*, 1142−1156.
(81) van Lenthe, E.; Baerends, E. J.; Snijders, J. G. *J. Chem. Phys.* **1993**, *99*, 4597−4610.
(82) van Lenthe, E.; Baerends, E. J.; Snijders, J. G. *J. Chem. Phys.* **1994**, *101*, 9783−9792.
(83) van Lenthe, E.; Ehlers, A.; Baerends, E.-J. *J. Chem. Phys.* **1999**, *110*, 8943−8953.
(84) Pye, C. C.; Ziegler, T. *Theor. Chem. Acc.* **1999**, *101*, 396−408.
(85) Raducan, M.; Rodriguez-Escrich, C.; Cambeiro, X. C.; Escudero-Adan, E. C.; Pericas, M. A.; Echavarren, A. M. *Chem. Commun.* **2011**, *47*, 4893−4895.